Geophys. J. Int. (2016) **206,** 557–573
Advance Access publication 2016 April 26
GJI Marine geosciences and applied geophysics
doi: 10.1093/gji/ggw167

Ground penetrating radar evaluation of the internal structure of fluvial tufa deposits (Dévanos-Añavieja system, NE Spain): an approach to different scales of heterogeneity

Ó. Pueyo Anchuela, A. Luzón, A. Pérez, A. Muñoz, M.J. Mayayo and H. Gil Garbi

Departamento de Ciencias de la Tierra, Univ. de Zaragoza. C/Pedro Cerbuna, nº 12. CP. 50.009. *Zaragoza, Spain. E-mail: opueyo@gmail.com*

Accepted 2016 April 22. Received 2016 April 22; in original form 2015 December 9

SUMMARY

The Quaternary Añavieja-Dévanos tufa system is located in the northern sector of the Iberian Chain. It has been previously tackled by means sedimentological studies focused on the available outcrops and some boreholes. They have permitted the proposal of a sedimentary scenario that fits with a pool-barrage fluvial tufa model. However a better knowledge of the characteristics and internal distribution of the usually non-outcropping pool deposits as well as of its relationship with barrage deposits has not been evaluated in detail yet. Palaeoenvironmental studies on tufas are usually biased because tufas are commonly delicate facies exposed to intense erosion during water level fall stages; for this reason outcrops are usually scarce and very often coincide with the most cemented barrage deposits. In order to analyse the internal characteristics of the tufa deposits under study, but also the lateral correlation among different facies, ground penetrating radar (GPR) has been employed both for the evaluation of its applicability in such kind of environments and to improve, if possible, the sedimentary model using geophysical data in sectors without outcrops. A GPR survey including different antennas ranging from 50 to 500 MHz along different sectors and its comparison with natural outcrops has been carried out. GPR results have permitted to deduce clear differences between pool and barrage deposits and to recognise its internal structure and geometrical relationships. The survey also permitted an approach to different scales of heterogeneities in the radarfacies evaluation by using distinct antennas and therefore, reaching different resolutions and penetrations. The resulting integration from different antennas allows three different attenuant and eight reflective radarfacies to be defined permitting a better approach to the real extension of the pool areas. These results have permitted to decipher the horizontal and vertical facies changes and the identification of a scarcer development of pool deposits than expected in the studied system.

Key words: Magnetic mineralogy and petrology; Sedimentary basin processes.

1 INTRODUCTION

The evaluation of geophysical methods in order to determine the internal structure of sedimentary bodies in both, sediments and rocks, is a common practice. ground penetrating radar (GPR), due to its resolution, has been usually applied at different contexts (e.g. aeolian dunes; Gawthorpe *et al.* 1993; Schenk *et al.* 1993; Bristow *et al.* 1996, 2000a,b; Van Dam 2002; marine para-glacial barriers systems; Van Heteren *et al.* 1998; fluvial environments Gawthorpe *et al.* 1993; Stephens 1994; Leclerc & Hickin 1997; Vandenberghe & van Overmeeren 1999; Pedley *et al.* 2000; Lunt *et al.* 2004; glacial deposits Olsen & Andreasen 1995; Haavisto-Hyvaerinen 1997; Busby & Marrit 1999; lakes; Jol & Smith 1991; Smith & Jol 1997; Craig *et al.* 2012; or channel-chenier structures; Weill *et al.* 2012).

The possibility to perform dense survey grids has permitted the evaluation in a more continuous and detailed manner and the construction of model facies at 2.5 and 3 dimensions (e.g. Bridge *et al.* 1995; Bristow 1995; McMechan *et al.* 1997; Anderson *et al.* 1999; Asprion & Aigner 1999; Beres *et al.* 1999; Pedley *et al.* 2000). The objectives of these works have been to correlate outcrops along not accessible sectors, to evaluate the homogeneous or heterogeneous correlations that can be obtained from isolated data and to perform detailed analysis aided by the resolution and meaning of the reflections at near outcrops.

In the case of carbonate rocks, GPR analysis has been applied mainly in the characterization of marine platform deposits (Pratt & Miall 1993; Liner & Liner 1995; Sigurdsson & Overgaard 1998; Asprion & Aigner 2000; Dagallier *et al.* 2000; Kruse *et al.* 2000; Collins *et al.* 2004; Asprion *et al.* 2009; Mukherjee *et al.* 2010;

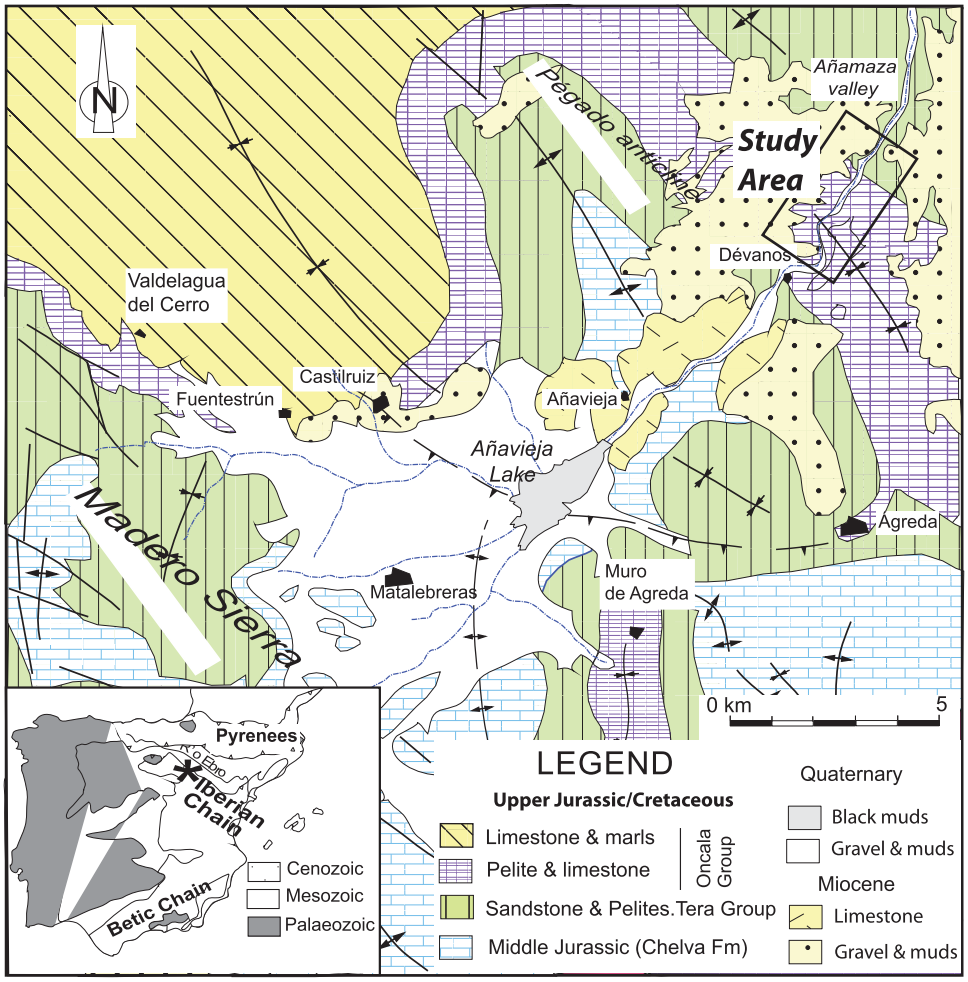

Figure 1. Geological context of the studied area. The location of the studied area is marked.

Jorry & Bievre 2011; Pueyo *et al.* 2012). At fluvial freshwater carbonates, the number of works are not scarce and geophysics has been applied to characterize thickness changes, 3-D reconstruction of sedimentological units, geophysical characterization, and determination of the bodies internal structure (e.g. Pedley 1993; Brusi *et al.* 1998; Hill *et al.* 1998; Pedley *et al.* 2000; Pedley & Hill 2003; Pedley 2009; McBride *et al.* 2012; Pérez *et al.* 2012). These works have been mainly performed on barrage/pools-dominated fluvial systems and have showed a high contrast between tufa barrage deposits and pool units. This contrast has permitted the evaluation of contacts between both types of units and the establishment of their map view distribution (Pedley 1993; Pedley *et al.* 2000).

Climate has been traditionally considered the main controlling factor on active tufa generation, which is especially favored during warm and wet episodes (e.g. Andreo *et al.* 1999; Horvatinčić *et al.* 2000; Pedley 2009). Nevertheless, climate conditions are not the only factor that affect the development of carbonate fluvial systems dynamics (Andrews *et al.* 1997, 2000; Kano *et al.* 2004; Andrews & Brasier 2005; Capezzuoli *et al.* 2010; Luzón *et al.* 2011) being needed to be considered also hydrological changes (Golubic 1969; Kano *et al.* 2007; Auqué *et al.* 2013), tectonic setting (Sbeinati *et al.* 2010; Ascione *et al.* 2014; Camuera *et al.* 2015) or the anthropogenic influence (Goudie *et al.* 1993; Limondin-Lozouet *et al.* 2010). Añavieja-Dévanos system was characterized during the Holocene interglaciar by stepped tufa barrages damming up small lakes or natural pools between them (Luzón *et al.* 2011; Fig. 1), and local cascades (Arenas *et al.* 2014).

In general, the analysed Holocene outcrops correspond to barrage deposits, with pool units scarcely outcropping and only identified by coring (Luzón *et al.* 2011). Moreover, farming activities complicate the establishment of the sedimentological system architecture in a continuous manner along the area. Pérez *et al.* (2012) performed a preliminary GPR survey in this system in order to evaluate its applicability at sectors without outcrops. These authors defined two main radarfacies (in terms of Baker 1991): a bright, reflective facies with high hyperbolic anomalies clustering against a second attenuant, non-reflective and more homogeneous facies. Both radarfacies have similar features to the previously identified by Pedley & Hill (2003) for tufa barrages and pool deposits respectively in other systems. As Carthew *et al.* (2003) suggested there is a persistence of hydraulic factors controlling the large-scale barrage dam-pool sequence, but at other scales and media, factors can differ. For this reason and due to the high contrasts identified along the preliminary geophysical survey in the Añamaza system, a more detailed analysis has been performed including GPR profiles over natural outcrops and along sectors where tufa deposits were expected to be present in the underground.

The objective of this more detailed second survey was to describe and interpret different scale radarfacies along the studied zone and to evaluate the possibility to use them to better establish the main

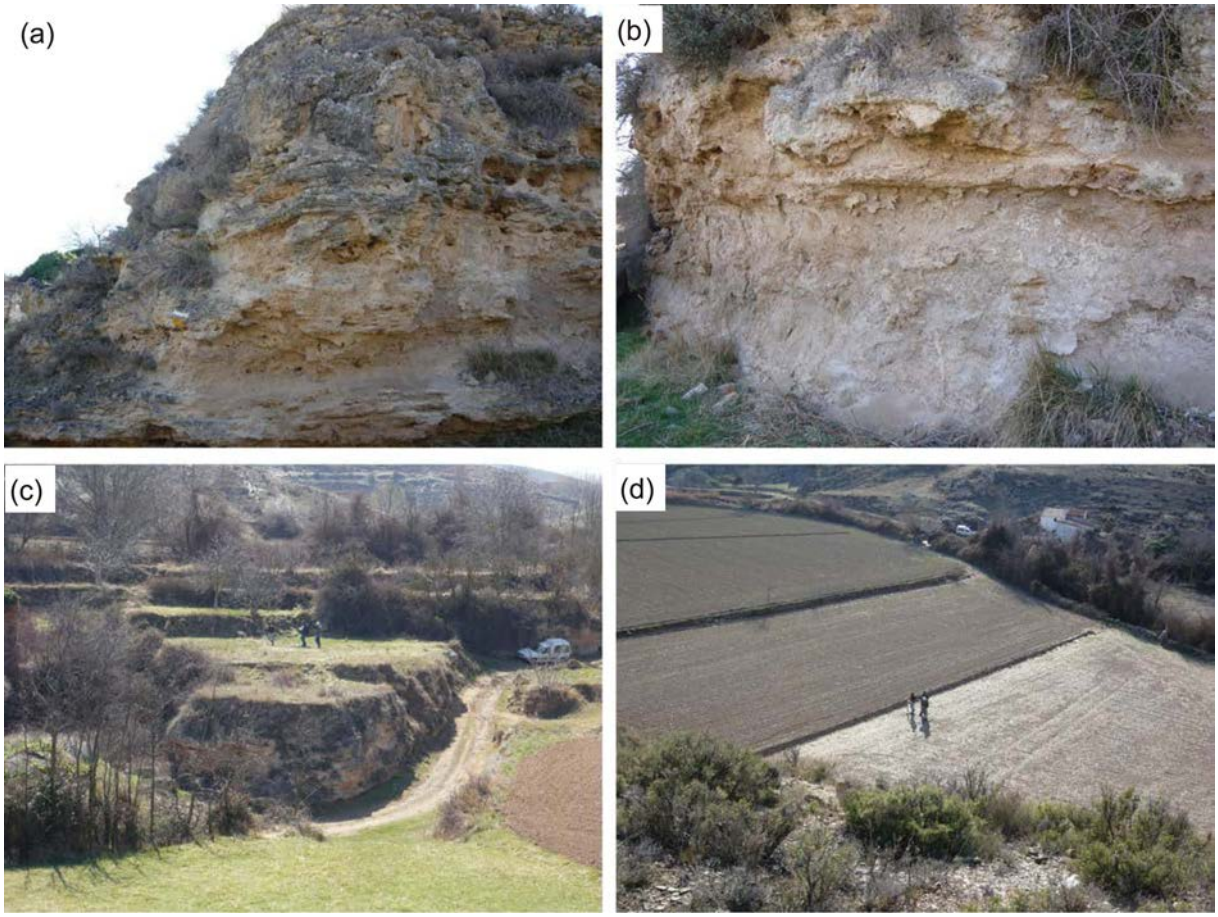

Figure 2. (a, b) Outcrops from the studied zone. (c, d) General aspect of the surveyed areas.

features and evolution of the sedimentary system. Different radarfacies have been defined attending reflectivity changes, structure and homogeneity, as well as through the integration of geophysical data. This evaluation has permitted to compare outcrops and profiles and the interpretation of GPR-profiles at sectors without tufa outcrops. Results provide a detailed characterization of the barrage-pool contacts both at the upstream and downstream face of the barrages. Moreover, the geometrical changes identified in the GPR-profiles, especially at the reflective (rich carbonate) media, have been interpreted in terms of sedimentological changes. A proposal of facies distribution in different horizontal planes along the surveyed zone has been also carried out and the sedimentary system evolution through time evaluated.

2 STUDY AREA

The Añamaza river valley is located in the central Iberian Range (Fig. 1). The geological succession in the region is mainly Mesozoic (Middle Jurassic-Lower Cretaceous) and Cenozoic in age (Fig. 1). The Mesozoic units are mainly carbonates (Middle Jurassic Chelva Formation; Gómez & Goy 1979; and Lower Cretaceous Oncala Group; Tischer 1965) that intercalate the detrital Tera Group (Jurassic-Cretaceous transition; Tischer 1965). Cenozoic conglomerates, mudstones and limestones lie subhorizontal and cover unconformably the Mesozoic succession. Several springs exist along the river valley, mainly located next to the Añavieja village. Groundwater supplies to the Añamaza River come from the Jurassic aquifer, with bicarbonate-sulphate calcium waters. Two main groups of springs can be identified (Coloma *et al.* 1996): those close to Añavieja village, at 960 m.a.s.l., and those located downstream, adjacent to Dévanos village, at 950 m.a.s.l. (Fig. 1).

Downstream Añavieja village, Quaternary deposits are mainly tufas. Among them, Holocene tufas are located slightly higher than the present river course and are the focus of this work. The fluvial barrage model described by Ford and Pedley (1996) and Pedley *et al.* (2000), fits well with the Holocene tufas in the Añamaza River, with barrages and dammed pool areas between them (Fig. 2), generated in a moderate-slope valley (Arenas *et al.* 2014). Although tufa outcrops are rarely higher than 8 m, more than 20-m-thick Holocene series has been preserved, as demonstrated by coring (Luzón *et al.* 2011; Pérez *et al.* 2012). The sedimentological features of the tufa deposits have been described with detail in previous works (Luzón *et al.* 2011; Arenas *et al.* 2014). Tufa barrages are dominated by highly porous carbonate facies, mainly phytoherm constructions, phytoclast and oncolite deposits; stromatolites are also frequent. Some intercalated levels of marls and sands with tufa remains and oncolites (wackestone to rudstone) also exist. Stagnant water (pool) deposits correspond to marls with oncolites and tufa debris, although cores drilled in these zones (Pérez *et al.* 2012) reveal that in pool areas decimetric levels of tufas can also exit. These are intercalated with mudstone and marl levels containing tufa debris and oncolites. Rich organic matter deposits are common, not only in the pool areas but also in adjacent peatland zones. Large flat areas used for agricultural purposes correspond to non-outcropping deposits made on carbonate sands and mudstones with common tufa

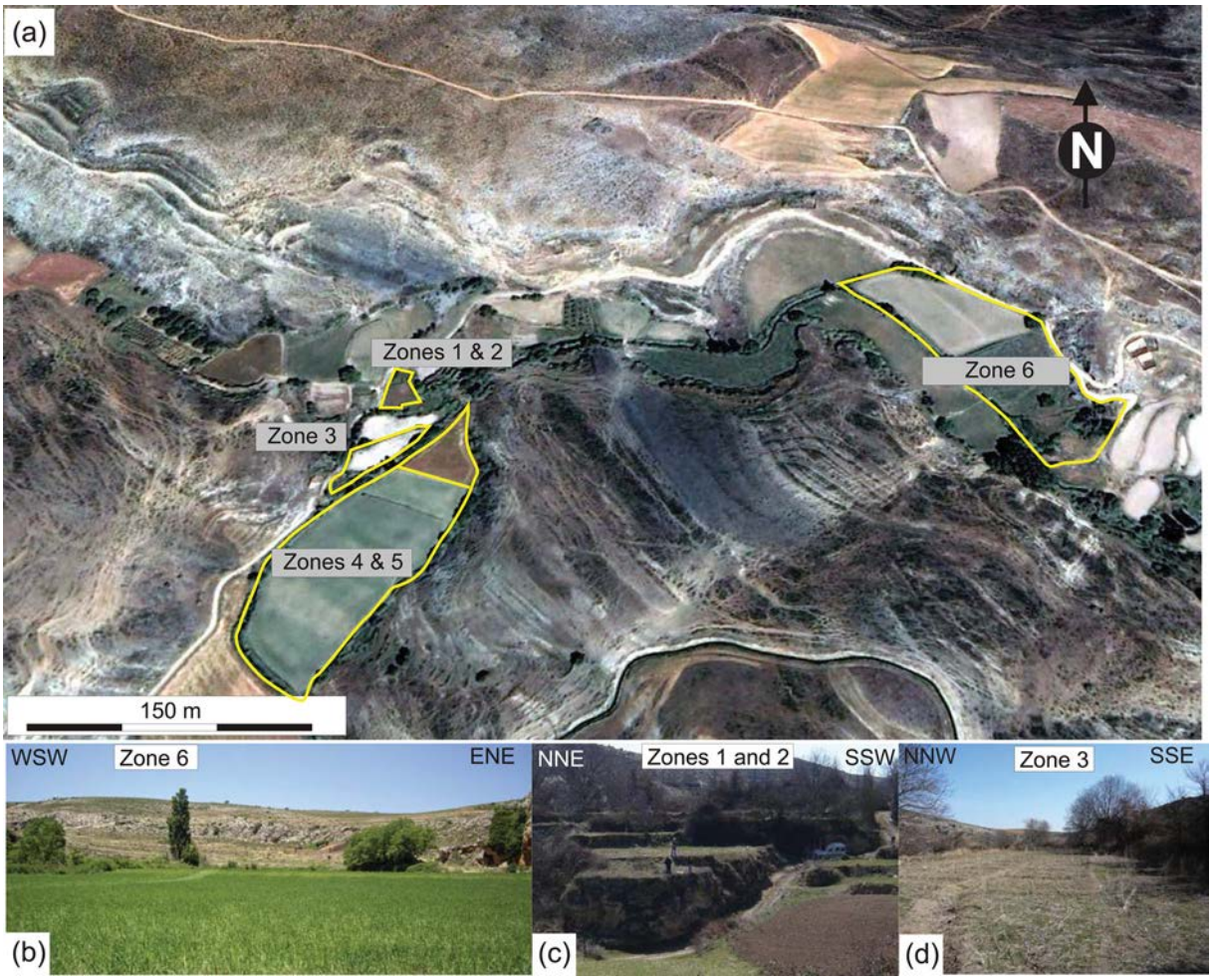

Figure 3. (a) Distribution of the studied zones. (b, c, d) Field aspect of the main surveyed zones including zones 6, 1 & 2 and 3.

debris and some intercalated phytoherm tufas (Luzón *et al.* 2011; Arenas *et al.* 2014).

3 GPR METHODOLOGY AND SURVEY

GPR is a geophysical technique based on the refraction, diffraction, reflection and scattering of electromagnetic (EM) waves in the underground. GPR results are dependent on the changes in the EM characteristics of underground deposits (dielectric permittivity, magnetic susceptibility and electrical conductivity) that are the origin of reflections on GPR profiles. In this sense, GPR permits the identification of changes of the underground structure. These changes are, in turn, dependent on the type and state of the soil. In this sense, the water content is one of the most significant influences on the EM impedance (e.g. Beres & Haeni 1991; Huggenberger 1993; Neal 2004). Moreover, the EM properties also depend on changes in grain size, clay content, pore-size and pore distribution, iron-oxides or organic matter content (Van Dam & Schlager 2000; Van Dam 2001).

A systematic GPR survey was performed in the Añamaza river valley over different morphological platforms and, in some cases, over outcrops where the stratigraphic features can be compared with the GPR results. GPR profiles were carried out at parallel and normal directions respect the current flow river direction and avoiding sharp topographical changes along profiles. As GPR-profiles were performed mainly along farming fields, the topography within each zone was subhorizontal (Fig. 3).

Preliminarily the survey was carried out with different GPR antennas in order to determine the resolution and penetration depth along the studied zone, as well as the most recommended antennas to be later systematically used. Six different survey zones were analysed through 120 profiles (8302 m of linear survey) with 4 different central frequency GPR antennas (unshielded 50 MHz and shielded: 100, 250 and 500 MHz; see Supporting Information for configuration survey and resolution from the carried out works). The comparison of GPR profiles and outcrops also collaborated in the selection of the central frequency used antennas. In this comparison, the identification of internal structural changes, good resolution and reflector definition, as well as penetration ranges, were considered. These data permitted to choose high frequency antennas as the most appropriated along the studied zone, including 250 and 500 MHz.

GPR wave propagation velocity was established by the modelling of diffraction hyperbolae at the GPR-profiles and direct comparison with natural outcrops. This analysis permitted to constrain a propagation velocity ranging from 78 to 113 m μs^{-1}. The mean value of propagation velocity and the comparison with two boreholes drilled in zone 6 permitted to establish a propagation velocity of 90 m μs^{-1} for the whole area (similar calculations have been obtained by Dagallier *et al.* 2000; Kruse *et al.* 2000; McBride *et al.* 2012). The use of an average value for time conversion and calculated data for propagation velocity are in the range of the obtained in

similar sedimentary settings by other authors, with values between 106 and 130 m μs^{-1} (Annan 1992; Neal 2004), average of 111 m μs^{-1} (Dagallier *et al.* 2000), caliche and other carbonate rocks with values between 60 and 50 m μs^{-1} (Kruse *et al.* 2000), 113 m μs^{-1} (Mukherjee *et al.* 2010), 70 m μs^{-1} at tufa deposits (Pedley & Hill 2003) or thermal tufas with average values of 90 m μs^{-1} (McBride *et al.* 2012).

Detailed GPR survey was configured based on the preliminary survey along the area, the identification of the penetration depth, and later configuration of TWT intervals at sectors with effective penetration (e.g. evaluation of the GPR profile characteristics and the identification of new reflections/diffractions in the underground as an indicator of real penetration). GPR data processing consisted on time-zero correction, filter of frequencies out of range for each device, running average to avoid irregular surficial displacement from the devices (resolution looses were reduced defining each trigger by 1024 samples and trig distances over the horizontal resolution for each central frequency; see Supporting Information). Exponential and linear gain was used to intensify GPR-waves at middle to depth conditions (below the skin depth), in some cases until GPR-wave saturation, and in others to constrain significant reflectors in the underground. Background removal and subtract mean trace procedures were also applied to try to erase the subhorizontal banded distribution of GPR-records.

4 RESULTS

4.1 Penetration, resolution and GPR antennas

As previously stated, GPR survey was carried out using different antennas along the same transects in order to evaluate resolution and penetration changes in the distinct surveyed areas. In general, penetration varies along the different prospected zones. These variations are not necessarily only related to the change in the central frequency of antennas. For example at zones 4 and 5, GPR penetration is similar with independence of the used antennas (50, 100, 250 and 500 MHz). In these areas penetration is conditioned by natural limits in the underground and it does not depend on the used antenna. It is interesting to note that unexpected 7 m of penetration were reached at, for example 500 and 50 MHz (e.g. zone 4 and 5; see Fig. 4). On the contrary, in other zones, penetration depends upon the used antennas, especially in the cases where reflective and attenuant media were identified during the survey. For example, at zone 6, penetration increases with the low frequency devices, and is dependent of the identified behaviour in subsurficial conditions (Fig. 5). In this sense, for all the used antennas, penetration is higher at reflective media while is limited at attenuant media.

These penetration changes suggest that if there were only reflective media, the reached penetration should be in the same range, with independence of the central frequency used, being advised the use of high frequency devices to obtain the highest resolution at such environments. On the other hand, at cases where attenuant media can be identified in the subsuperficial zone or inferred from the GPR records in depth, the penetration is limited by these levels, which act as conductive barriers that preclude higher penetrations. These changes between reflective and attenuant media permitted to define, in a similar manner than Pedley (1993) and Pérez *et al.* (2012), the presence of two main radarfacies along the studied area: radarfacies 1 and 2. Radarfacies 1 (R1) is characterized by attenuant, non-reflective behaviours, limited penetration, and scarce reflectors with general subhorizontal or low-slope attitude. Radarfacies 2 (R2) is characterized by reflective behaviours, high penetration, well-defined reflectors, cluster of hyperbolic anomalies that in some cases is defined by their coalescence and general non-homogeneous horizontal reflector distribution.

4.2 Distribution of reflector changes between and within different radarfacies

The two radarfacies are not uniformly distributed along the studied zones. In fact, R1 was only identified at zone 6. In the rest of the cases, attending the same processing routine applied to GPR-profiles, the surveyed zones coincide with reflective media (R2). The contrast expected between both radarfacies in terms of propagation velocity and penetration should define a net contact of wave propagation in the underground. On the contrary the detailed analysis carried out at zone 6 over the contact between both radarfacies, reveals a non-homogeneous transition (Fig. 6; zone 6). R1 and R2 are related laterally by net contacts and subvertical changes or by a progressive adaptation. In this zone, several parallel profiles permitted the distribution of facies to be constructed for different discrete depth intervals, as well as to evaluate the extension of each radarfacies. This procedure permitted to identify changes in the geometrical relation between both radarfacies along the survey direction (Fig. 6) that coincides, in turn, with the flow direction.

If the internal structure and geometry of the deposits is considered, besides a simple distinction based on reflectivity and attenuation changes, a more detailed classification of facies can be proposed. A summary of the geometrical changes identified along the whole studied zone is included at Fig. 7 where both radarfacies types can be subclassified attending to their internal structure. This classification takes into account the most commonly identified geometrical changes along the studied zone, without considering its potential sedimentological interpretation. In this sense the highest complexity is identified at R2 facies.

Within R1, that presents a more homogeneous and attenuant behaviour, none or very scarce reflectors were identified. When present, they usually show horizontal or low-sloped contacts. Attending to the internal structure, three radarfacies subtypes have been defined. The differences between them are related to: (i) the identification of horizontal attenuated and homogeneous distribution (R1A), (ii) the presence of progressive-lateral accommodations within R1 facies (R1B) or (iii) the development of homogeneous sectors with hyperbolic anomalies, usually related to the presence of R2 behaviours within R1 (R1C).

For R2, due to the higher penetration and better definition of the reflectors, more radarfacies subtypes were established. In the analysed case, including data along the whole surveyed zone, eight different reflective subradarfacies have been differentiated attending, mainly, to the geometrical characteristics and lateral continuity of the reflectors (Fig. 7). R2A consists on accommodated reflectors that show continuous distributions; R2B is similar to R2A but reflectors are not laterally continuous (they show truncations and heterogeneous behaviours). R2C is defined by a high concentration of hyperbolic anomalies being difficult to separate reflectors from the hyperbolic branches. R2D is characterized by usually well-defined convex-plane geometries in 2-D sections. R2E shows accommodations that define plane-concave or channel geometries but includes more complex geometrical changes than R2C. Radarfacies R2D presents a relative increase of reflectivity that it is also identified at R2F. In the later, it can be observed a vertical development of

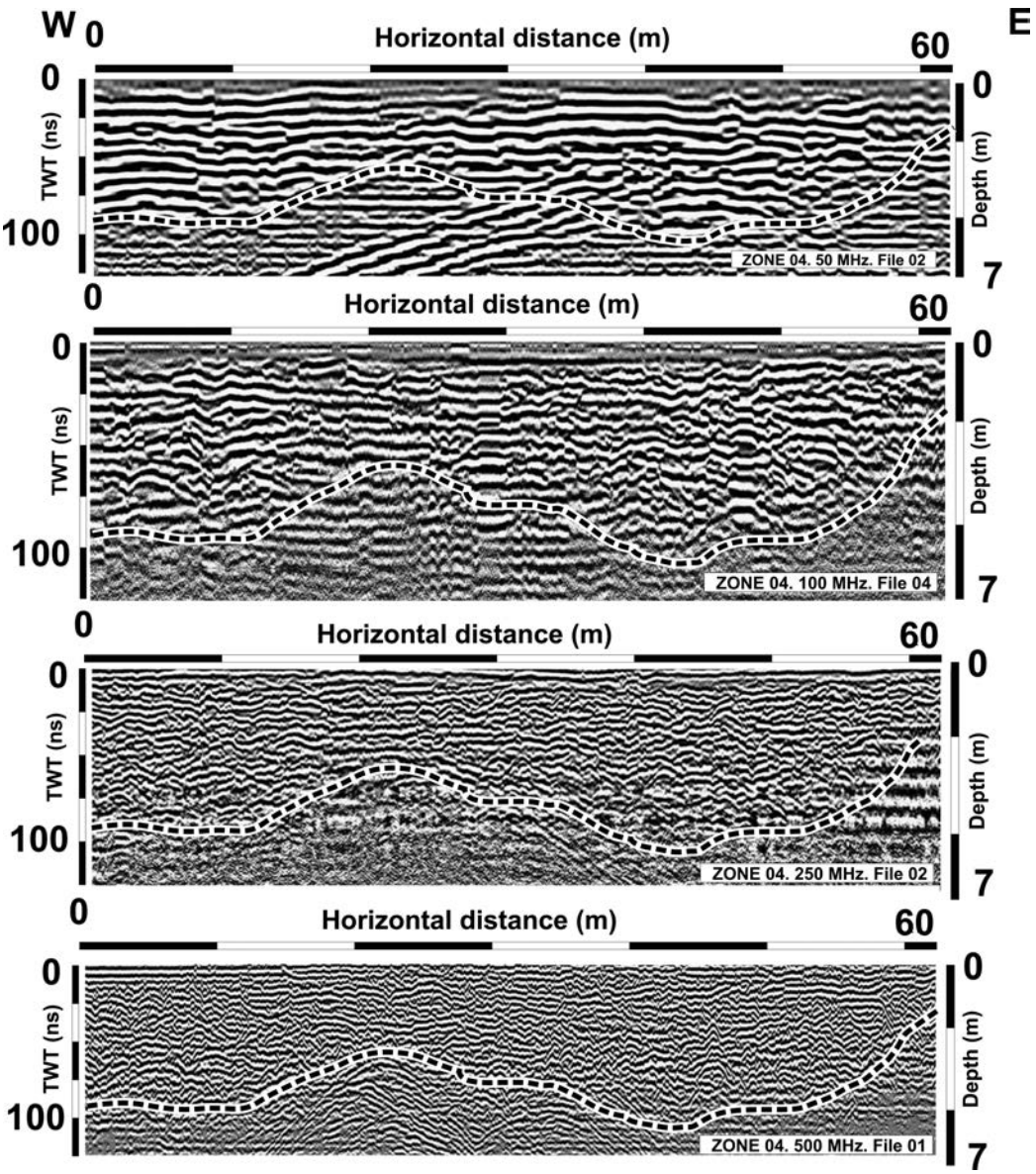

Figure 4. GPR profiles carried out along the same transect with different central frequency antennas. Over the profiles a line that is considered the limit of penetration along the profiles is also marked. In the eastern sector from the profiles it can be observed the outcropping of Jurassic units that is interpreted as the net contact in the GPR penetration in the underground.

reflective media related to a hyperbolic, or cluster of hyperbolic anomalies. R2G and R2H represent domains with geometrical changes where lateral accommodation is identified through defined homogeneous trends and low-sloped attitudes (usually accommodating to a previous lower surface) but R2H is more homogeneous, and it presents parallel and continuous reflectors in the underground. This facies has been only identified at the upper part of the GPR profiles.

In order to evaluate both, radarfacies changes and obtained results at the studied area, an example of the used methodology is included at Fig. 8. In this figure profiles made on two normal directions and with different antennas are included. Whether the internal characterization is considered, a reflective media (R2) with numerous hyperbolic and plane-concave geometries can be identified. NNW–SSE profiles, normal to the expected main flow direction, show abrupt lateral changes of thickness in relation to the reflective media (R2) that nearly disappears in the northern sector, towards the lateral edge of the carbonate system at the contact with the Mesozoic succession. The comparison between 250 and 100 MHz antennas for this domain permits to identify a similar reached penetration depth for both antennas whereas the resolution of both profiles depends upon the used antenna. The WSW–ENE profile (Fig. 8) is parallel to the expected flow-direction, and many of the previously proposed subradarfacies can be identified on it. In general, homogeneous, low-sloped and accommodated geometries are identified for the most surficial conditions, which contrast with the geometries located below them that show higher lateral variability, accommodated and convex-plane geometries, vertical propagation of anomalies and reflective media with high anomaly clusters. Homogeneous sectors in the deepest zones from the profiles can be related both to the loose of resolution with depth or the presence of more homogeneous facies. These lower units are laterally interrupted by the development of vertical anomalies and convex-plane geometries.

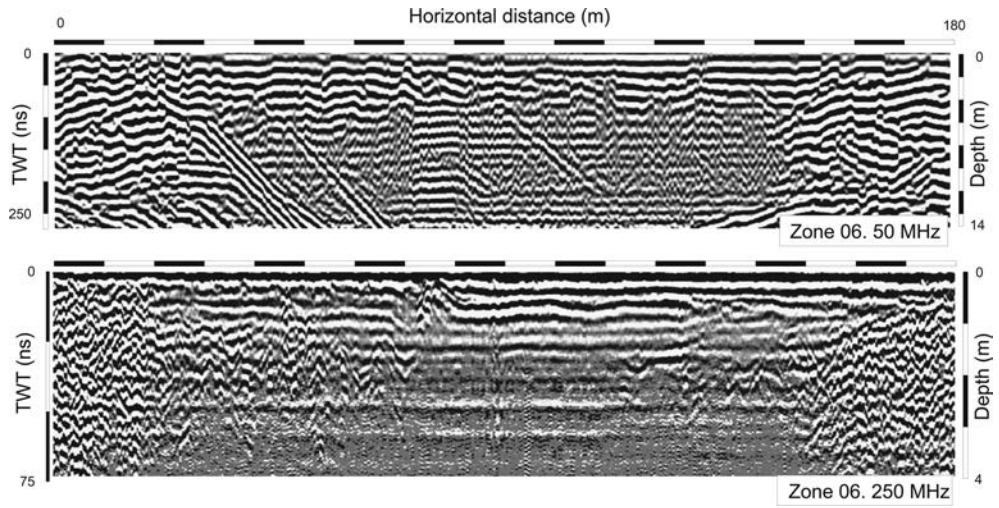

Figure 5. Examples of profiles from zone 6 where it can be observed the change in penetration for 50 and 250 MHz profiles and the change between reflective and attenuant media.

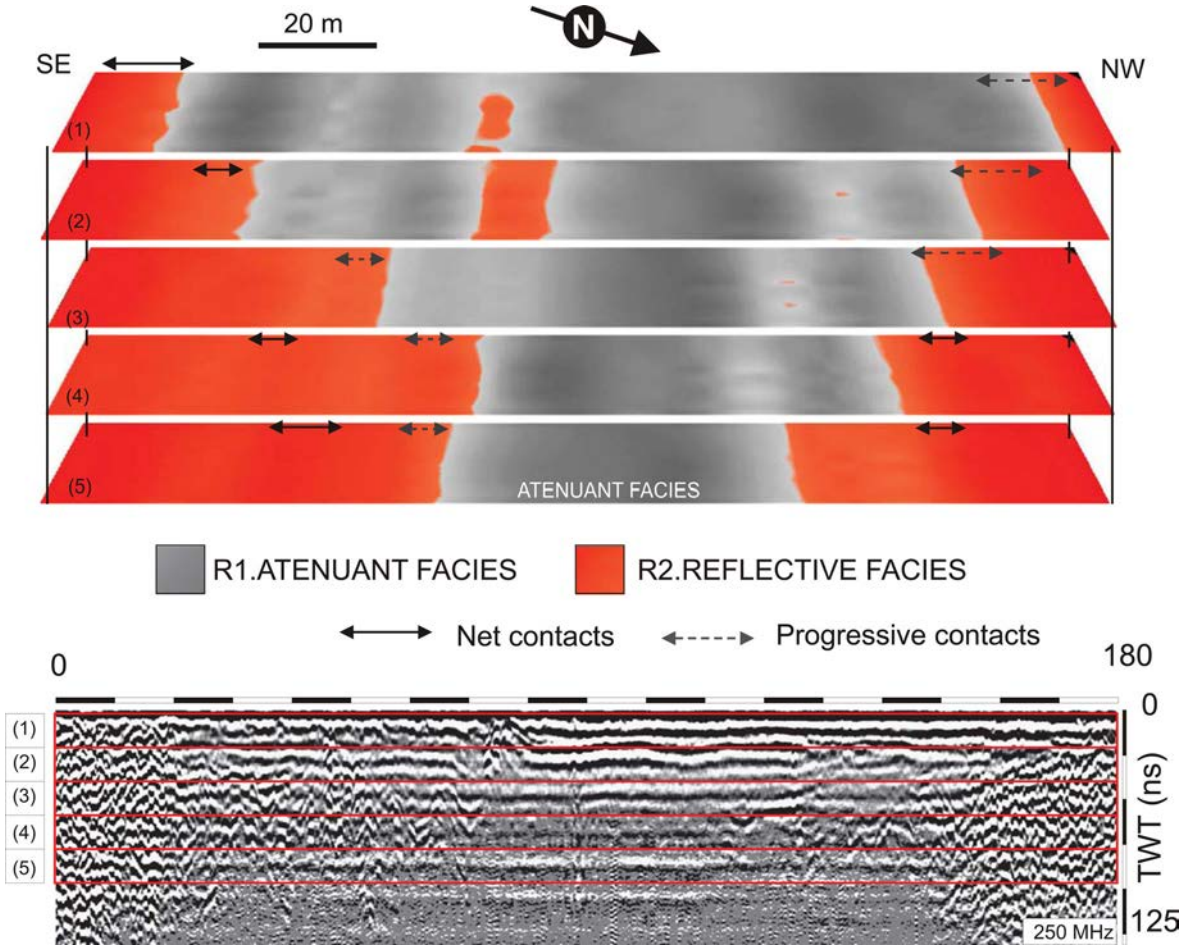

Figure 6. Main distribution of reflective and attenuant media along survey zone 6. Model has been established considered the main reflective and attenuant media for different TWT-depth intervals. Along the upper plots the distribution between reflective and attenuant facies and the reference to the progressive and net changes between both units are also marked. Note that the analysed intervals are included at the left part of the GPR-profile.

Although mostly of the subradarfacies can be identified in this profile, their precise contacts are not always evident and their lateral extension has not been identified in terms of defined reflectors. In this sense, it is easier to evaluate the distribution of radarfacies both at the profile and the map view, than to precisely establish the extension of such units. In order to perform a more detailed analysis of the subradarfacies distribution, a map view evaluation similar than the performed at zone 6 (Fig. 6), has been carried out at Fig. 9. Map view distribution of facies along different temporal intervals (two-way traveltime; TWT) in the studied zone has

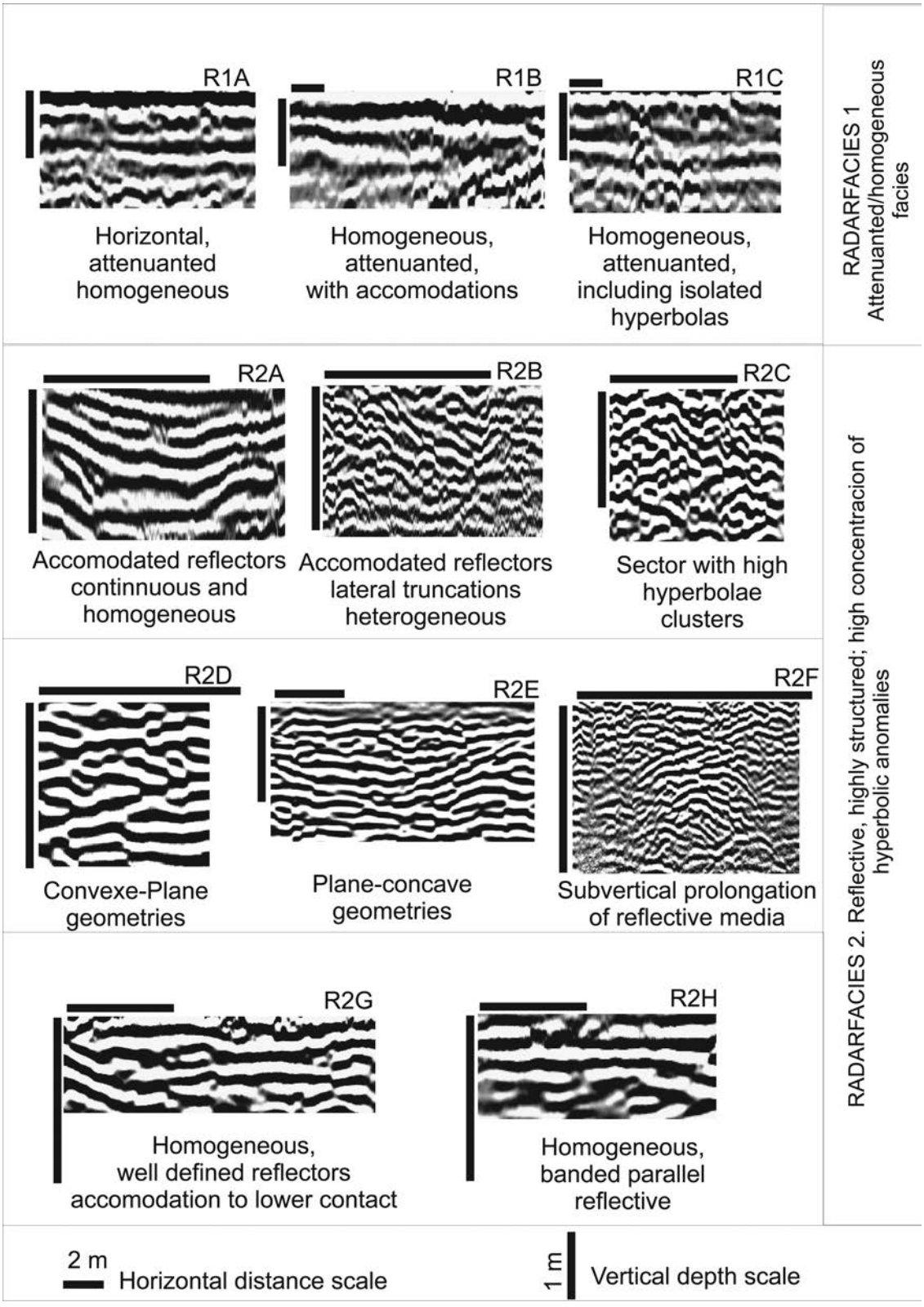

Figure 7. Main identified radarfacies along the whole studied zone. Classification considers reflective versus attenuant behaviours. Later within each one of the behaviours, subclassification of radarfacies has been done attending structural changes. The main structural characteristics are also included at the figure (see text for full description). Vertical and horizontal scale from different radarfacies are different, the same scale has been included in order to evaluate its horizontal and vertical distribution.

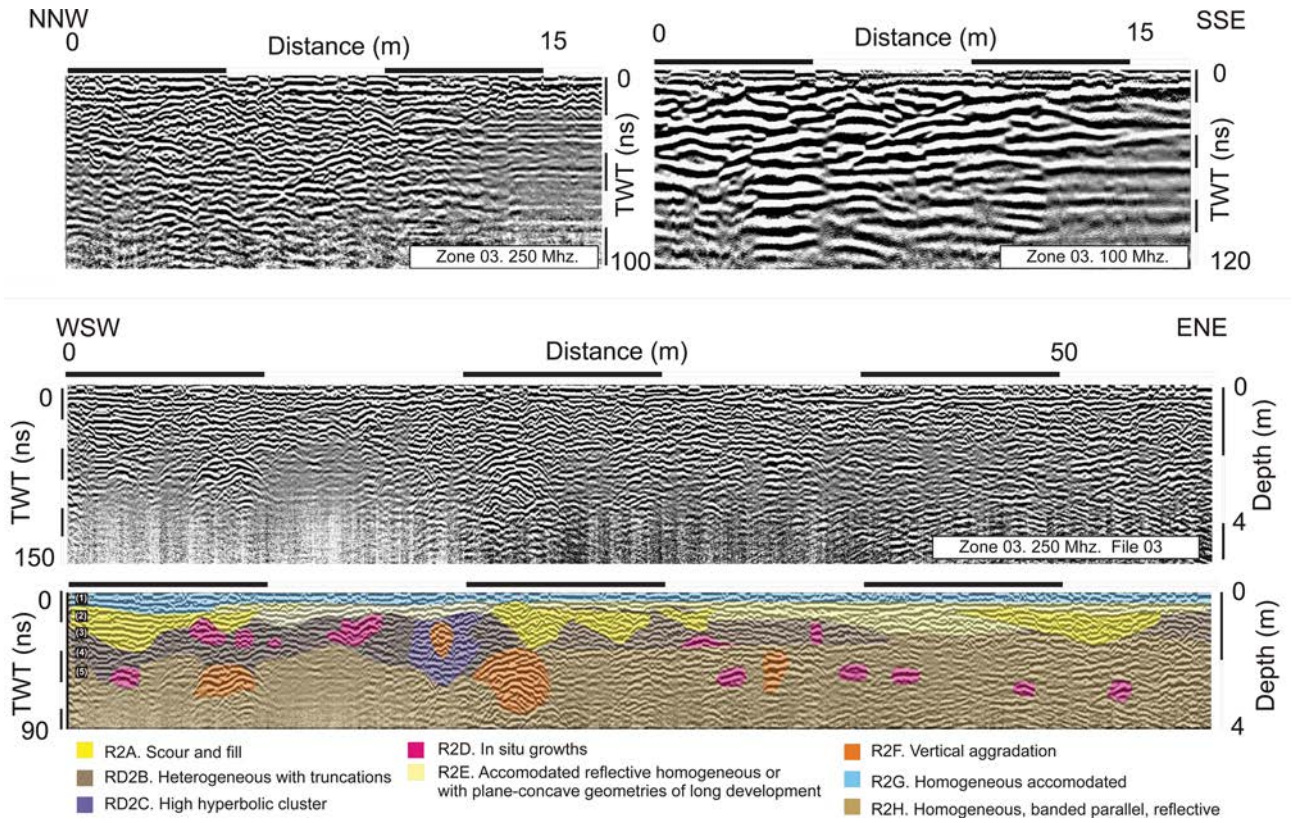

Figure 8. GPR profiles along survey zone 3. Profiles from 100 and 250 MHz are included in order to be compared. Normal profile from 250 MHz is included and where radarfacies units have been identified (the horizontal lines from lower plot represents the intervals where radarfacies distribution map has been carried out at Fig. 9).

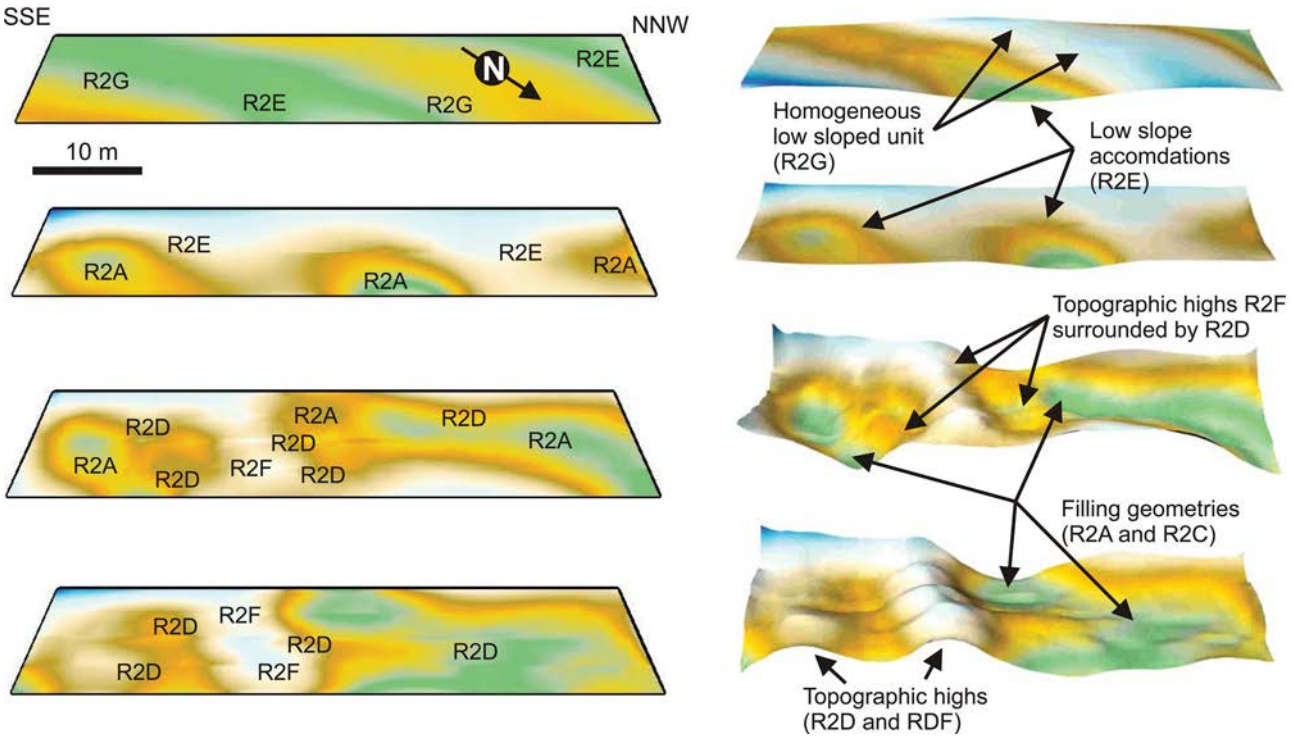

Figure 9. Distribution of facies obtained from the analysis of GPR profile included at Fig. 8. Map view and false-relief images are included for the 4 analysed intervals. See Fig. 8 for depth location.

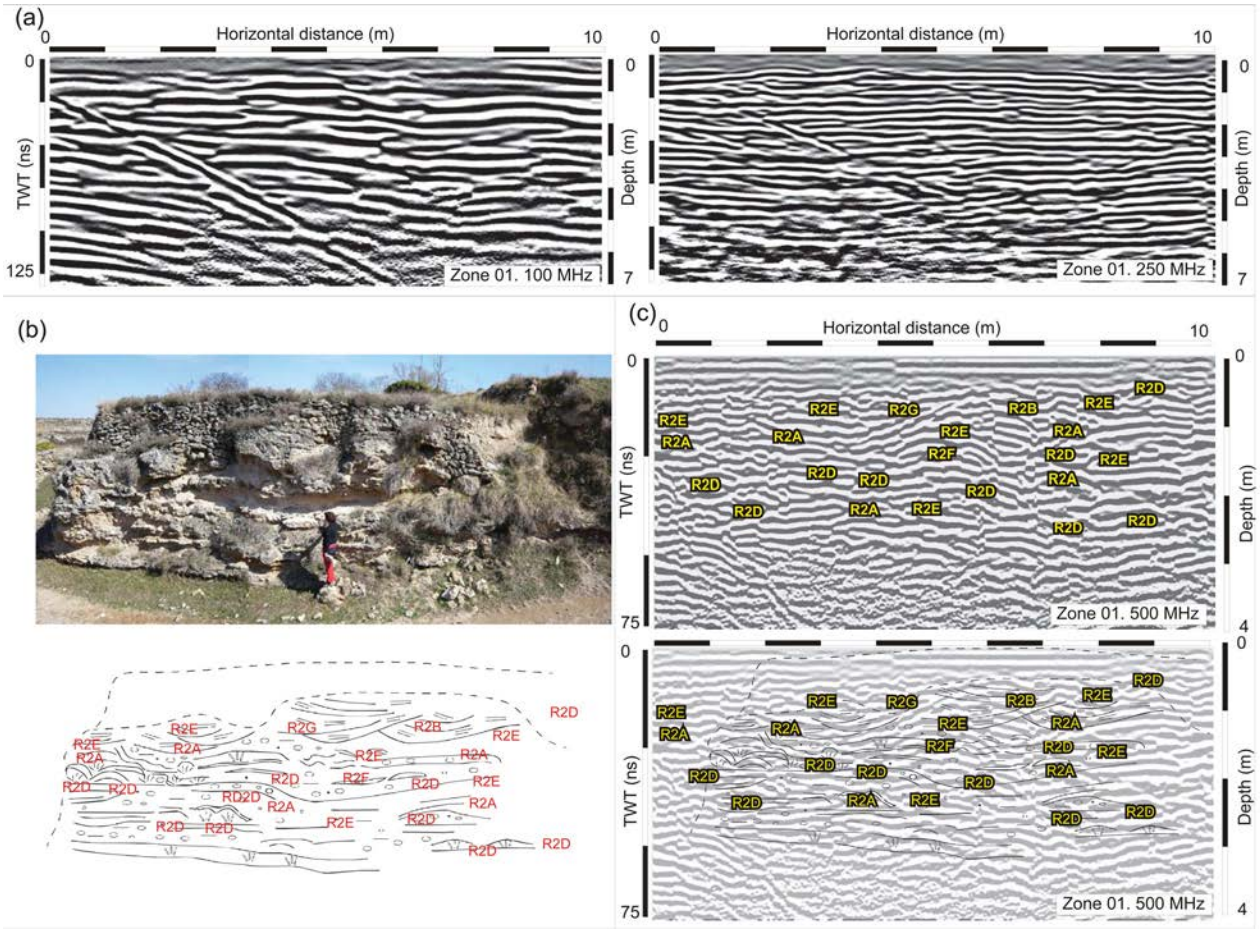

Figure 10. Compared analysis of outcrop and GPR profiles including different central frequencies antennas. (a) Different GPR profiles done with 100 and 250 MHz antennas are displayed. (b) Outcrop photograph and sedimentological line sketch of the analysed exposure. (c) Superposition of identified radarfacies and geometrical changes identified at the outcrop over the GPR-profile of 500 MHz. Note the clear correlation between radarfacies and sedimentological characteristics but the low availability to identify, in all of the cases, the limits between sedimentological units through isolated reflectors.

permitted to correlate subradarfacies in different depth intervals and to evaluate their distribution by integrating different parallel and normal profiles. From top to bottom a shallow unit with homogeneous characteristics is identified (R2G and R2E) that presents progressive reflector changes and low-sloped contacts. Below this upper unit, homogeneous units (R2E and R2A facies) and a higher complexity in the internal structure is identified. The relation between both units consists on general accommodation geometries with changes in the vertical development and reflectors slope. The highest thickness and geometrical complexity is identified at R2A facies. Downwards, the same radarfacies are still identified producing topographical positive geometries along the area. In this interval R2A appears within R2F and R2D. In general, the stronger topographical changes are related to R2F facies, and usually R2D is identified isolated within more homogeneous units, or bordering R2A facies. The map view distribution and the integration of different parallel and normal profiles permits to correlate R2A facies to channel geometries in 2-D section, which progress along different profiles from the area. The deepest units are again defined as more homogeneous respect the upper ones, and R2H facies are laterally interrupted by R2F and R2D facies and where the top of R2H defines an irregular topography.

4.3 Comparison of outcrops and GPR-profiles and defined radarfacies

At some sectors in the studied zone there exist outcrops in which a comparison between GPR profiles and sedimentological features can be established (Fig. 10a). Usually exposures do not permit to evaluate more than 4 m depth. A comparison between the outcrop and GPR profiles was performed at survey zone 1 (Fig. 10), with different antennas in order to evaluate penetration and resolution. The clearest identified reflector (Fig. 10a) is the aerial anomaly related to the lateral termination of the surveyed zone over the topographic platform (see Fig. 2 for survey location). Beside this anomaly, other minor changes can be identified with low resolution at the 100 MHz profile. The highest resolution with a similar penetration depth is identified at the case of 250 and 500 MHz.

Zone 1 is mainly reflective in agreement with the dominant carbonate lithology (Figs 2, 10b and 11). Different reflectors, and their continuity, can be observed and analysed. The main lateral changes are defined by net interruptions or by general accommodation geometries. However, from a geometrical point of view, not all the identified stratigraphic levels produce defined reflectors at the GPR profiles. At the case of the 500 MHz (Fig. 10c), a clear correspondence can be observed between stratigraphic levels at outcrop and

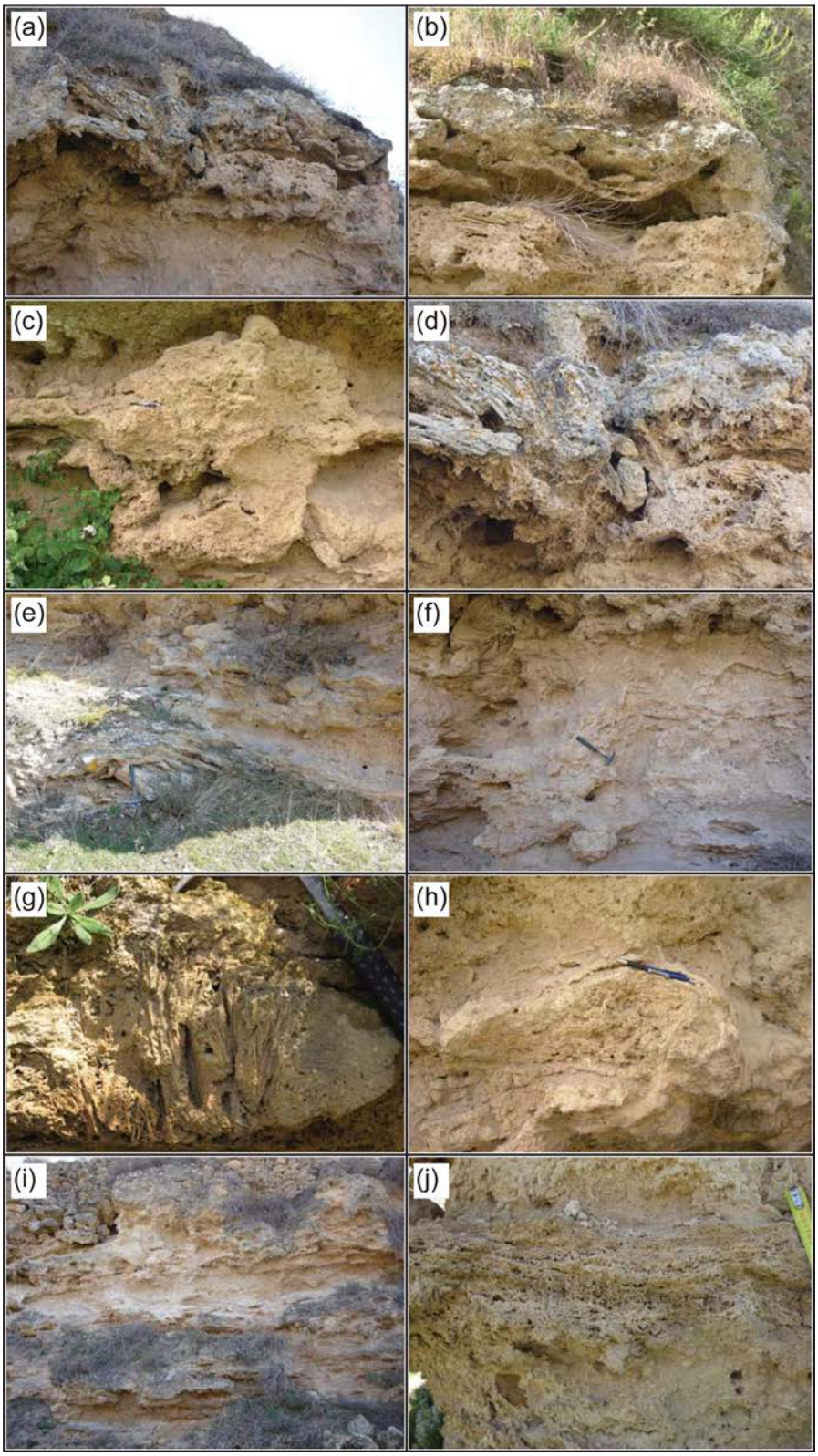

Figure 11. Photographs from outcrops from the studied area. Different structural and textual units similar to the identified structures in the GPR-profiles are included. (a) Channel tufa geometries in the upper part of the outcrop contrast with the tabular and more terrigenous bodies in the lower part. (b, c, d) represent concave up geometries. (b) corresponds to a channel filled with crossed stems, (c) to a phytoherm, and (d) shows a eroded level of coated stems filled with heterogeneous facies. (e) Smooth channel geometry (towards the right of the photo). (f) Cross-section of a step made of tufa in the bottom of the fluvial area (probably related to a very small cascade). (g, h) Small phytoherms. (i, j) General view and detail of alternating tabular decimetre-thick levels made on tufa debris and tufa constructions.

reflectors, especially when they are not horizontal, as mainly occurs in the upper part.

On the other hand, the comparison of data from exposures with different profiles carried out with different central frequency antennas permits to evaluate different resolution and detail in the evaluation of GPR profiles depending the required resolution, detail and sedimentological meaning. By one hand, different detail can be achieved where high resolution profiles permits to evaluate small structures and geometrical changes within the units, while the identification of the overall sedimentary architecture can be difficult to be achieved. On the other hand, the evaluation at middle to low resolution antennas permits to identify the thickness of the Quaternary units, its general architecture but it is not able to perform the characterization of the internal structure or identified facies in the outcrop. In this sense, the integrated information from different antennas permits to recognise different scales from the heterogeneity of the studied materials.

In this sense, the correspondence is very clear for the cases where plane-concave geometries exist, which correspond with different channel fill deposits (Figs 10c and 11a) mainly located in the upper part of the outcrop. The exact contact that separates every domain is not always clear and the channel geometries can be hardly laterally delimited at the profiles. Therefore, the descriptive assignation of radarfacies permits to evaluate similar geometrical characteristics in the outcrop but, in some cases, the extent of radarfacies cannot be as detailed delimited as in the outcrop.

For the analysed case and with the objective to evaluate the similarities between the sedimentological characteristics of the outcrop and the GPR results, some considerations can be established. From one hand the plane-concave geometries are defined through radarfacies that were described in function of reflector accommodations. In general, plane concave geometries observed in the outcrop correlate with R2A, R2B, R2C and R2E radarfacies defining channelled bodies. When a more precise interpretation can be done, R2A represent progressive filling of shallow channels (Fig. 11b). R2B and C are also channelled deposits but related to more massive fillings (Figs 11c and d) and R2E corresponds to wide slightly concave upwards deposits that can be related to wider channels, a more longitudinal section, or a stepped bottom if profile is parallel to the expected flow direction (Figs 11e and f). In this zone, and attending to the lateral distribution of reflectors, its truncation or accommodation, it can be generally observed a progression from R2E at the lower part to R2A at the upper part. The most upper units show a higher lateral reflector continuity that widely progress over the in-depth plane-concave geometry. R2B and R2C are usually associated with these geometries, while they present a progression from R2E, R2C and R2A over them. This progression is not always identified, and in some cases, only some of the radarfacies can be identified showing the highly heterogeneity of facies in the carbonate fluvial system. In other cases, such radarfacies can be identified isolated without relation with the rest of radarfacies. Radarfacies R2G and R2H are identified at the upper part of the profile, related with the recent soils and facies that finally cover expansively the carbonate system, or laterally to the rest of units along the whole analysed system.

In the lower part of the deposit geometrical changes permitted two main groups of radarfacies to be identified, considering either the presence of convex-plane geometries (R2D) or vertical propagation of reflective media (R2F). For the case of the studied outcrop at Fig. 10(a), both radarfacies correlate with phytoherms with different vertical distribution and size. R2D correlates with isolated clusters of in situ growths of stems (Figs 11g and h) or domes of bryophytes, and R2F with wider structures or, in this case, with bryophyte phytoherms (Fig. 11h). In both cases, net contacts exist with respect the surrounding units in the lower part (R2H) and R2G units adapt and overlap R2D and R2F facies.

Phytoherms correlate to high reflective media along the profiles, which in some cases produce vertical propagation of anomalies below the real position at the outcrop. Considering the direct comparison between both datasets, these anomalies can be interpreted in terms of the coalescence of vertical growths, carbonate precipitation or sudden lateral net changes of the sedimentary structure. Homogeneous units, in this comparison, reveal that horizontal or homogeneous units do not show clear reflectors in the profiles. In contrast, not horizontal levels or lateral slope changes are clearly defined in the GPR profiles.

5 DISCUSSION

5.1 Meaning of defined radarfacies in terms of sedimentological characteristics

One of the objectives of the performed comparison and analysis was to identify the different geophysical signatures of tufa facies at GPR profiles and to evaluate if the reflectivity and geometrical changes can be used in terms of prediction of the sedimentological facies in the underground. This evaluation, in case of the identification of structural representative signatures, could permit to propose sedimentological interpretations for those sectors where no accessibility exists, but where similar structural changes or radarfacies can be identified univocally in the underground. In summary, this possibility should permit to increase the knowledge of these erodible systems, to improve the 3-D distribution along the area and to refine models at sectors with limited accessibility.

From a preliminary point of view, a definition of the main groups of radarfacies has been performed along the studied zone just considering reflectivity changes between units. Geometrical and geophysical features of R1 and R2 facies (Figs 5 and 6) permit to interpret them as pool and barrage deposits, respectively. Barrage buildings are separated by subhorizontal reflectors (Fig. 5) that indicate a low depositional slope. These results, similar to the proposed for carbonate barrage deposits and sapropelmarly pool units by Pedley & Hill (2003) or Pérez *et al.* (2012), have permitted not only to determine in which sectors pools and barrage deposits exist in the underground, but also to characterize their lateral contacts and lithology. As pool deposits are very erodible they are scarcely preserved and usually masked below agricultural soils where prediction can be limited. The direct analysis, through trenches for example, is also limited due to the presence of a near water level (between 0.5 and 2 m at the studied area). The survey along different sectors where the presence of this kind of deposits in the Añavieja-Dévanos system was expected, has permitted to infer for them a low representation, being only identified in one of the analysed sectors. Reflective facies dominate in the system and this suggests a higher presence of continuous carbonate levels than lacustrine mud deposits that was not the expected situation in low slope areas. These tabular levels are identified in outcrops as composed by detrital tufas, stems bunches and lying stems (Figs 11i and j) and represent the deposition of tufa debris in pools during common episodes of erosion of the barrages located upstream, or marginal deposits of channel or dammed areas where vegetation grew.

The transition between both elements (barrage and pool), from a preliminary geophysical point of view, can generate variations

in the propagation velocity and reflectivity that produce apparent geometrical changes in the profiles not related with real geometrical in the deposits. The analysis has been performed determining a mean propagation velocity along the area (obtained from hyperbolic fitting, boreholes and outcrops). The comparison of geometrical changes between the main radarfacies and outcrop features indicates that the change of propagation velocity is not the origin of such geometrical variations and they follow the sedimentological and structural geometries of the analysed units.

In this sense, the evaluation carried out at zone 6 has permitted to compare the geometrical relations between both sedimentological elements and to infer from these geometries the expected facies progression. By one hand, the extension of R1 and R2, or pool and barrage units, presents two variation trends: vertical and horizontal. In general, lateral relationships between the pool areas (R1) and barrages (R2) are more progressive in the upstream face of the barrage (Figs 5 and 6). On the contrary higher interdigitation between such facies is recognised in the downstream face of the barrages that is related to the existence of stepped barrages. This progression slightly varies if the analysis is carried out for different TWT-depth intervals where both, net contacts and progressive steeped progressions can be identified. The facies distributions show that R1 facies extension is more limited at depth than at the surface. R1 facies shows vertical net contacts or slightly overlapping geometries over R2, and R2 progresses at downstream positions. At the southern limit (upstream position) the contact between R1 and R2 is usually more progressive and R1 overlaps R2. This overlapping can be identified by the progressive displacement of the R1 limit towards the south, and the development of different on lap geometries. In terms of compared analysis of sedimentology and geophysical geometries, the identified structural facies distribution can be interpreted as an increase of wideness of the pool media with time (more expansive in the upper part of the series). This increase happened due to the vertical growth of the downstream barrier and the on-lapping of the pool deposits in the downstream side of the barrage located upstream, suggesting a forced onlap of the pool sediments. This general facies distribution improves the sedimentological interpretation, as outcrops are not available to evaluate the actual origin and geometrical disposition between pool and barrier deposits.

Attending to the internal structure, different subradarfacies have been described for R1 and R2. In R1, three radarfacies subtypes (R1A, R1B and R1C) can be defined. As previously indicated, they are considered to represent pools or areas with slow water flow where horizontal levels of marls with tufa remains, alternate with tufa levels (e.g. stem levels, oncolites or detrital tufa). This data has been identified at the cores drilled in the area (DV2 from Pérez *et al.* 2012). R1A represents the central part of the pool, whereas R1B, with progressive-lateral accommodations is located at the contact between R1 and R2, that is to say, represents the pool-barrage contact. R1C is interpreted as related to tufa constructions (e.g. phytoherms) in the marginal areas of the pool area, or in more central parts but during low water level episodes.

For the case of R2, a higher number of subfacies have been distinguished. An attempt to correlate them with the outcropping sedimentary facies has been made. This comparison show that R2A accommodated reflectors with continuous distribution could represent progressive filling channels, whereas truncations and heterogeneous behaviours in R2B indicate a more heterogeneous facies. R2B has not been identified in the outcrop of Zone 1 but it could be related to the existence of carbonate boulders, blocks or coalescent phytoherms filling a channelled area that have been identified in neighbouring outcrops. R2C is defined by a high concentration of hyperbolic anomalies that suggests a massive, non-structured media where different types of facies and geometries (perhaps phytoherms) can be very close each other. R2E is related to wide channel shapes or fillings of previously stepped areas. Well-defined 2-D convex-plane geometries in R2D and R2F have been correlated to phytoherm constructions, but R2F shows a vertical development of the reflective media related to a hyperbolic, or cluster of hyperbolic anomalies, suggesting a wider carbonate building similar to a small tufa barrage. Finally, R2G and R2H represent defined homogeneous trends and low-sloped attitudes (usually accommodating to a previous lower surface). They have been identified in the uppermost part and represent tabular and continuous levels of tufa facies filling shallow areas between barrage constructions; they correspond to pool deposits but with a high content of detrital tufas.

Whether R2 facies is dominant, the distribution of radarfacies (Figs 8 and 9) permits to obtain different map views at different depths and temporal moments in the system evolution. This approach has been evaluated considering different TWT intervals (depth; or vertical variations during time). The evaluation of the different radarfacies signatures and its direct comparison with outcrops permit to determine the sedimentological characteristics of the studied radarfacies. The internal characterization of perpendicular profiles at Fig. 8, with numerous hyperbolic and plane-concave geometries, indicates that they were made over a barrage area. Its disposition with respect the present river course and geometry suggest that one profile (SSE–NNW) is parallel to the river flow whereas the other one is perpendicular to it. This implies that the former is perpendicular and the latter parallel to the barrage construction. ENE–WSW profiles, normal to the expected main flow direction, show abrupt lateral changes of thickness in the eastern sectors, towards the lateral edge of the carbonate system and the contact with the Mesozoic succession.

Within R2 facies, as identified at the studied zone 3 at shallow conditions, R2G and R2E dominate (progressive reflector changes and low-sloped contacts). Below them, R2E and R2A facies suggest a higher complexity, with accommodated geometries and changes in the vertical development and reflectors slope. In the deepest part, more homogeneous facies exist (R2H) that are laterally interrupted by R2F and R2D facies. The evaluation of the geophysical signatures and their compared analysis with exposures, support a general homogeneous unit that is laterally interrupted by plane-concave geometries representing scour and fill, channel, deposits. Units also adapt to phytoherms and stromatolites and other accumulations of carbonate elements (tufa debris or oncolites). The distribution of these net changes shows that the margin of phytoherms (R2D) usually progresses surrounding scour and fill geometries. The upper units usually progress in onlap over phytoherms (homogeneous facies surrounding and adapting to subvertical elements of high reflective contrasts related to R2F facies).

The evaluation of these geometries in combination with the sedimentological meaning permits to identify a vertical variation of the studied environments represented by different facies correlations (Figs 9 and 12). A deeper and older zone (interval 1) characterized by an irregular topography where topographic highs defined by R2D and R2F facies delimit other sectors with accommodation and plane-concave geometries in 2-D section (R2D facies) that can be followed along different profiles. At middle depths (interval 2), a change is identified with the appearing of incision geometries (plane-concave geometries related to lateral interruptions of the continuity of the reflectors) interpreted as scour and fill geometries (e.g. R2A, R2B or R2E) affecting to homogeneous media where the incision and scour geometries show a more irregular topography.

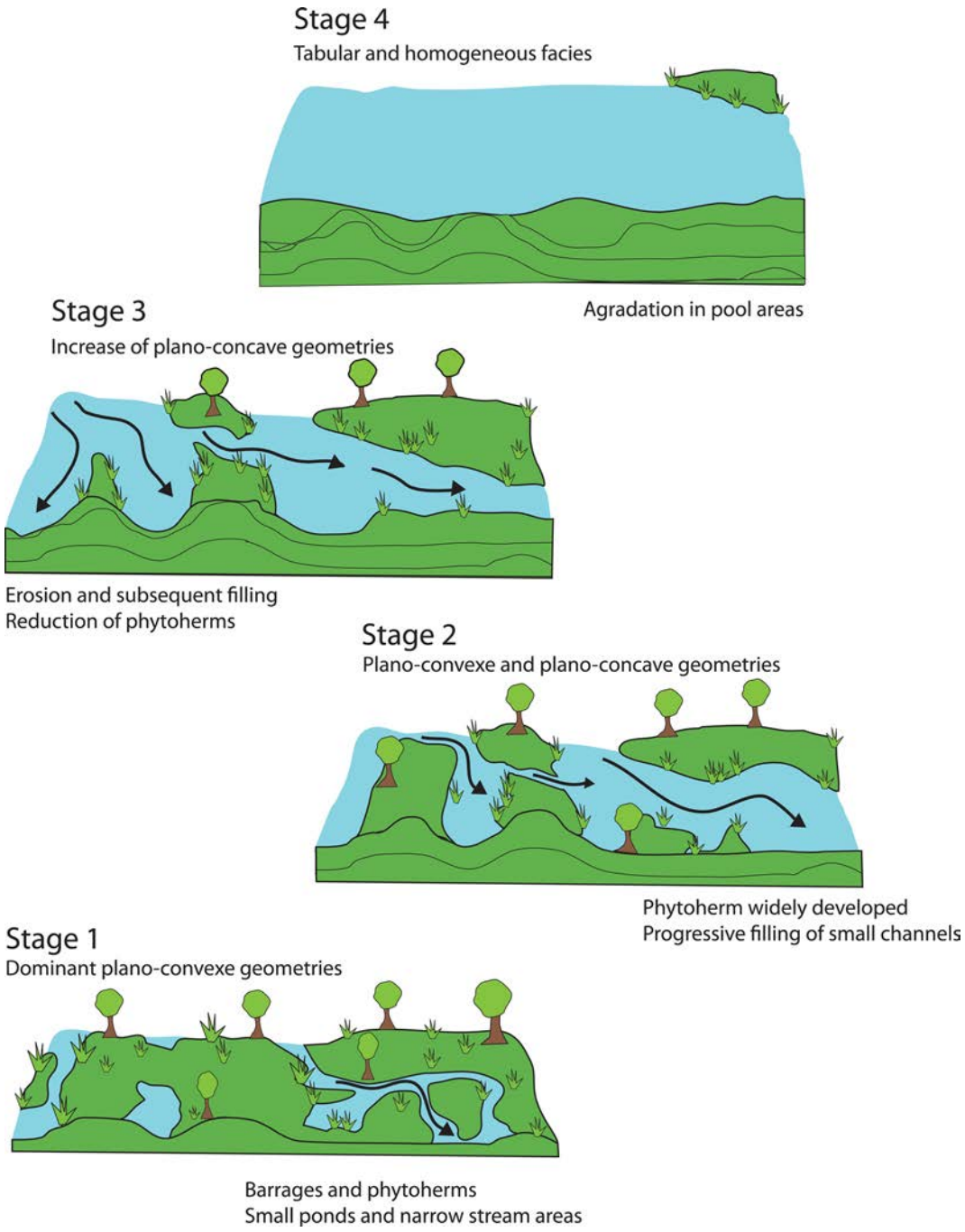

Figure 12. Palaeoenvironmental evolution of zone 3 and interpretation of the main changes in terms of sedimentological and environmental changes.

In this system also relative topographic highs related to R2D and R2F facies exists. However, the main origin of the topographical changes is related to the incision and erosion and later sedimentation accommodating to these geometries. Internally these sectors can present: zones with laterally continuous reflectors (R2A), irregular fills (R2B), non-continuous reflectors in the plane-concave geometries (R2E) and upper units overlapping these topographical changes with low sloped reflectors (e.g. R2G). The upper 3rd interval is related to a more homogeneous topography. In this stage R2G and R2H are mainly identified. The main structural changes are related to small accommodations and R2D facies distribution is limited. A similar distribution with more homogeneous reflector trends is identified at the uppermost interval (4).

These geometrical changes can be interpreted in terms of sedimentological variations along the studied system and where scour and fill geometries and vertical carbonate growths configured the sedimentation space. In general, scour and fill geometries, but also the progressive aggradation trends, define the sedimentation space (Fig. 12). Carbonate growths (phytoherms) are absent in the uppermost interval where only low-sloped geometries are identified. This upper interval correlates with oncolite and tufa debris deposits that progress upwards into the agricultural soils identified in the surface and at the analysed accessible outcrops. In summary, different stages can be inferred for this area (Figs 9 and 12): an initial scenario corresponding to the existence of carbonate buildings laterally related to flooded areas where tabular tufa bodies, calcified stems

levels or detrital tufas dominate. Over them, and laterally related to them, channel and plane-convex geometries suggest a second scenario dominated by channels, perhaps related to an incision stage, and phytoherm constructions. Erosion persisted during a third stage where carbonate buildings do not exist. Finally, the channels were filled and a system with tufa horizontal levels developed, that is interpreted as a return to aggrading conditions when pools were filled by detrital tufas. It must be notice that the general evolution resembles in a general manner to the inferred at zone 1. Dating from Arenas *et al.* (2014) indicated a possible hiatus included between 7.7 and 3.3 Ka BP, which could have been related to the erosive, channel dominated stage inferred in zone 3.

The integrated analysis has permitted to identify pool and barrage media in the underground, to correlate isolated outcrops and to evaluate the internal structural changes in the underground from geophysical data. This evaluation has permitted, for example, the identification of small barrages inside the pools (Fig. 6) or to detect local incision and subsequent aggradation inside a given barrage. Moreover the study shows that, in the first case, the small bioconstructions inside the pools can be laterally connected with large barrages, a very relevant aspect when the connectivity of porous facies is taken into consideration, as occurs in hydrocarbon reservoirs. Other features related to the contacts between pools and barrages, more progressive in the downstream face of the barrages and more vertical in the upstream face, had not been analysed in detail previously, and reveal high connectivity between porous tufa levels in pools and large barrages in the downstream direction.

On the other hand the evaluation of facies changes along different vertical intervals has permitted the identification that the top of the barrage located downstream is topographically higher than that upstream (Fig. 6). This evidence an aggrading system changing from a barrage dominated scenario to another one in which pool areas widened, suggesting a local base level change (Fig. 12). Arenas *et al.* (2014) proposed a double sedimentological framework for this area: a moderate and a high-slope fluvial model. These two were laterally related and interpreted as associated, respectively, to moderate and high slope reaches of the valley. In our case, the vertical evolution inferred by GPR survey suggest that a change from high to moderate slope model could happen in the same point during the Holocene, almost locally (as in zone 6), due to local damming. In this sense RB architecture reflects a geometry dependent of the available space with pool sediments in the upper part of the succession onlapping and covering barrages.

6 CONCLUSIONS

GPR survey along the Dévanos-Añavieja carbonate fluvial system has been carried out in order to evaluate the possibility to determine structural changes that can be evaluated in terms of sedimentological architecture of the tufa deposits. This evaluation has permitted to confirm the existence of two main behaviours referring to barrier and pool deposits and where, in the studied case, such changes mainly refers to the structural particle pattern moreover than the own mineralogy. In both contexts the deposits are mainly carbonates, even in the pool environments, dominated by tufa debris, small phytoherms and oncolites. This feature permits to evaluate that the carbonatic cementation, growth of the deposits and their texture has a higher imprint in the geophysical record than the chemical or mineralogical characteristics.

The geophysical internal changes within barrage deposits have permitted to identify scour and fill geometries, aggradation and growth progressions, the lateral relations between different units and the temporal evolution of the studied system. These changes have been analysed together with outcrops in order to validate the application of such methodologies in the improvement of sedimentological studies focused on this kind of deposits. Moreover, the internal analysis of the scour and fill geometries permits to study the vertical progression of their filling and the presence of well-defined anomalies in correlation to phytoherms, phytoclasts or stromatolites that configured the sedimentation spaces. The use of different groups of GPR antennas has permitted to identify, depending on the potential resolution of GPR, different scales of heterogeneity that have permitted to evaluate the sedimentological system progression with different resolution, detail and evaluation scale.

The exact identification of the limits between different sedimentary bodies has not been clearly established from GPR, possibly because their similar geophysical signature. However the identification of radarfacies features and their horizontal and vertical distribution has permitted the evaluation of the lateral (spatial) and vertical (temporal) system progression.

The presented results support the interest of integrated analysis of GPR with sedimentological data at available outcrops and their joint interpretation along sectors without direct exposures. This procedure has permitted a better reconstruction of the ancient sedimentological environments related to barrage and pool deposits.

ACKNOWLEDGEMENTS

This research has been financed by project CGL2009-09 165/BTE from Spanish Science Ministry, Feder funds and Research Groups from Aragon Government ‘Análisis de Cuencas Sedimentarias Continentales’ and ‘Geotransfer’ (UZ-DGA). Authors want to acknowledge the comments and suggestions from editor Petrovsky and two anonymous reviewers.

REFERENCES

Anderson, M.P., Aiken, J.S., Webb, E.K. & Michleson, D.M., 1999. Sedimentology and hydrogeology of two braided stream deposits, *Sediment. Geol.*, **129,** 187–199.

Andreo, B., Martín-Martín, M. & Martin Algarra, A., 1999. Hydrochemistry of spring water associated with travertines. Examples of the Sierra de la Alfaguara (Granada, southern Spain). Comptes Rendus de l’Academie des Sciences Paris, *Sciences de la Terre et des Planètes*, **328,** 745–750.

Andrews, J.E. & Brasier, A.T., 2005. Seasonal records of climatic change in annually laminated tufas: short review and future prospects, *J. Quarter. Sci.*, **20,** 411–421.

Andrews, J.E., Riding, R. & Dennis, P.F., 1997. The stable isotope record of environmental and climatic signals in modern terrestrial microbial carbonates from Europe, *Palaeogeogr. Palaeoclimatol. Palaeoecol.*, **129,** 171–189.

Andrews, J.E., Pedley, M. & Dennis, P.F., 2000. Palaeoenvironmental records in Holocene Spanish tufas: a stable isotope approach in search of reliable climatic archives, *Sedimentology*, **47,** 961–978.

Annan, A.P., 1992. Ground Penetrating Radar Workshop Notes, Sensors and Software, Ontario, Canada.

Arenas, C., Vázquez-Urbez, M., Pardo, G. & Sancho, C., 2014. Sedimentology and depositional architecture of tufas deposited in stepped fluvial systems of changing slope: lessons from the Quaternary Añamaza valley (Iberian Range, Spain), *Sedimentology*, **61,** 133–171.

Ascione, A., lannace, A., Imbriale, P., Santangelo, N. & Santo, A., 2014. Tufa and travertines of southern Italy: deep-seated, fault-related CO_2 as the key control in precipitation, *Terra Nova*, **26,** 1–13.

Asprion, U. & Aigner, T., 1999. Towards realistic aquifer models: three-dimensional georadar surveys of Quaternary gravel deltas (Singen Basin, SW Germany), *Sediment. Geol.*, **129,** 281–297.

Asprion, U. & Aigner, T., 2000. An initial attempt to map carbonate buildups using ground-penetrating radar: an example from the Upper Jurassic of SW-Germany, *Facies*, **42,** 245–252.

Asprion, U., Westphal, H., Niemanm, M. & Pomar, L., 2009. Extrapolation of depositional geometries of the Menorcan Miocene carbonate ramp with ground penetrating radar, *Facies*, **55,** 37–46.

Auqué, L.F., Arenas, C., Osácar, C., Pardo, G., Sancho, C. & Vázquez Urbez, M., 2013. Tufa sedimentation in changing hydrological conditions: the River Mesa (Spain), *Geol. Acta*, **11,** 85–102.

Baker, P.L., 1991. Response of ground penetrating radar to bounding surfaces and lithofacies variations in sand barrier sequences, *Expl. Geophys.*, **22,** 19–22.

Beres, M. & Haeni, F.P., 1991. Application of ground-penetrating radar methods in hydrogeologic studies, *Ground Water*, **29**(3), 375–386.

Beres, M., Huggenberger, P., Green, A.G. & Horstmeyer, H., 1999. Using two and three dimensional georradar methods to characterize glaciofluvial architecture, *Sediment. Geol.*, **129,** 1–24.

Bridge, J.S., Alexander, J., Collier, R.E.L., Gawthorpe, R.L. & Javiers, L., 1995. Ground penetrating radar and coring used to study the large-scale structure of point bar deposits in three dimensions, *Sedimentology*, **42,** 839–852.

Bristow, C.S., 1995. Internal geometry of ancient tidal bedforms revealed using GPR, *Int. Assoc. Sedimentol.*, **24,** 313–328.

Bristow, C.S., Pugh, J. & Goodall, T., 1996. Internal structure of aeolian dunes in Abu Dhabi determined using ground-penetrating radar, *Sedimentology*, **43,** 278–320.

Bristow, C.S., Bailey, S.D. & Lancaster, N., 2000a. The sedimentary structure of linear sand dunes, *Nature*, **406,** 56–59.

Bristow, C.S., Chroston, P.N. & Bailey, S.D., 2000b. The structure and development of foredunes on a locally prograding coast: insights from ground penetrating radar surveys, Norfolk, UK, *Sedimentology* **47,** 923–944.

Brusi, D., Palli, L., Roque, C., Capella, I., Pujadas, A. & Vehi, M., 1998. Geophysical lectromagnetic prospection in the spatial location of the travertine deposits of the Banyoles depression (Girona). Geological and hydrological implications, in *Proc. Environ. Eng. Geophys. Soc*., Barcelona, 1998 September 3, pp. 205–208.

Busby, J.P. & Merritt, J.W., 1999. Quaternary deformation mapping with ground penetrating radar, *J. appl. Geophys.*, **41**(1), 75–91.

Camuera, J., Alonso-Zarza, A.M., Rodríguez-Berriguete, A. & Meléndez, A., 2015. Variations of fluvial tufa sub-environments in a tectonically active basin, Pleistocene Teruel Basin, NE Spain, *Sediment. Geol.*, **330,** 47–58.

Capezzuoli, E., Gandin, A. & Sandrelli, F., 2010. Calcareous tufa as indicators of climatic variability: a case study from southern Tuscany (Italy), *Geol. Soc. Lond. Spec. Publ.*, **336,** 263–281.

Carthew, K.D., Taylor, M.P. & Drysdale, R.N., 2003. Are current models of tufa sedimentary environments applicable to tropical systems? A case study from the Gregory River, *Sediment. Geol.*, **162,** 199–218.

Collins, M.E., Cum, M. & Hanninnen, P., 2004. Using ground penetrating radar to investigate a subsurface karst landscape in north-central Florida, *Geoderma*, **61,** 1–15.

Coloma, P., Martínez Gil, F.J. & Sánchez Navarro, J.A., 1996. La laguna de Añavieja. Funcionamiento y génesis, *Geogaceta*, **20,** 1258–1260.

Craig, M.S., Jol, H.M., Teitler, L. & Warnke, D.A., 2012. Geophysical surveys of a pluvial lake barrier deposit, Beatty Junction, Death Valley, California, USA, *Sediment. Geol.*, **269–270,** 28–36.

Dagallier, G., Laitinen, A., Malartre, F., Van Campenhout, I.P.A.M. & Veeken, P.C.H., 2000. Ground penetrating radar application in a shallow marine Oxfordian limestone sequence located on the eastern flank of the Paris Basin, NE, France, *Sediment. Geol.*, **130,** 149–165.

Ford, T.D. & Pedley, H.M., 1996. A review of tufa and travertine deposits of the word, *Earth Sci. Rev.*, **41,** 117–175.

Gawthorpe, R.I., Collier, R.E.I., Alexander, J., Leeder, M.R. & Bridge, J.S., 1993. Ground penetrating radar: application to sandbody geometry and heterogeneity studies, in *Characterisation of Fluvial and Aeolian Reservoirs*, pp. 421–432, eds North, C.P. & Prosser, D.J., Geological Socierty of London.

Golubić, S., 1969. Cyclic and noncyclic mechanisms in the formation of travertine, *Verhandlungen der international Vereinigüng für Limnologie*, **17,** 956–961.

Gómez, J.J. & Goy, A., 1979. Las unidades litoestratigráficas del Jurásico medio y superior, en facies carbonatadas del Sector Levantino de la Cordillera Ibérica, *Est. geol.*, **35,** 569–598.

Goudie, A.S., Viles, A. & Pentecost, H.A., 1993. The late-Holocene tufa decline in Europe, *Holocene*, **3,** 181–186.

Haavisto-Hyvaerinen, M., 1997. Pre-crag ridges in southwestern Finland, *Sediment. Geol.*, **111**(3/4), 147–159.

Hill, I., Pedley, H.M. & Denton, P., 1998. GPR, GPS and Promax, applied to the detailed sedimentary architecture of tufa deposits, in *Proc. Environ. Eng. Geophys. Soc*., Sept. 1998, Barcelona, pp. 433–437.

Horvatinčić, N., Čalić, R. & Geyh, M.A., 2000. Interglacial growth of tufa in Croatia, *Quat. Res.*, **53,** 185–195.

Huggenberger, P., 1993. Radar facies: recognition of facies patterns and heterogeneities within Pleistocene Rhine Gravels, NE Switzerland, in *Braided Rivers*, Vol. 75, pp. 163–176, eds Best, J.L. & Bristow, C.S., Geological Society of London.

Jol, H.M. & Smith, D.G., 1991. Ground penetrating radar of northern lacustrine deltas, *Can. J. Earth Sci.*, **28,** 1939–1947.

Jorry, S.J. & Biévre, G., 2011. Integration of sedimentology and ground-penetrating radar for high-resolution imaging of a carbonate platform, *Sedimentology*, **58,** 1370–1390.

Kano, A., Tatsuya Kawai, T., Matsuoka, J. & Ihara, T., 2004. High-resolution records of rainfall events from clay bands in tufa, *Geology*, **32,** 793–796.

Kano, A., Hagiwara, R., Kawai, T., Hori, M. & Matsuoka, J., 2007. Climatic conditions and hydrological change recorded in a high-resolution stable-isotope profile of a recent laminated tufa on a subtropical island, southern Japan, *J. Sediment. Res.*, **77,** 59–67.

Kruse, S.E., Schneider, J.C., Campagna, D.J., Inman, J.A. & Hickey, T.D., 2000. Ground Penetrating radar imaging of cap rock, caliche and carbonate strata, *J. appl. Geophys.*, **43,** 239–249.

Leclerc, R.F. & Hickin, E.J., 1997. The internal structure of scrolled floodplain deposits based on ground penetrating radar, North Thompson river, British Columbia, *Geomorphology*, **21,** 17–38.

Limondin-Lozouet, N. *et al.*, 2010. Oldest evidence of Acheulean occupation in the Upper Seine valley (France) from an MIS 11 tufa at La Celle, *Quat. Int.*, **223–224,** 299–311.

Liner, C.L. & Liner, J.L., 1995. Ground-penetrating radar: a near-face experience from Washington County, Arkansas, *Leading Edge*, **14,** 17–21.

Lunt, I.A., Bridge, J.S. & Tye, R.S. 2004. A quantitative, three-dimensional model of gravelly braided rivers, *Sedimentology*, **51,** 377–414.

Luzón, A., Pérez, A., Borrego, A.G., Mayayo, M.J. & Soria, A.R., 2011. Interrelated continental sedimentary environments in the central Iberian Range (Spain): facies characterisation and main palaeoenvironmental changes during the Holocene, *Sediment. Geol.*, **239,** 87–103.

McBride, J.H., Guthrie, W.S., Faust, D.L. & Nelson, S.T., 2012. A structural study of thermal tufas using ground-penetrating radar, *J. appl. Geophys.*, **81,** 38–47.

McMechan, G.A., Gaynor, G.C. & Szerbiak, R.B., 1997. Use of ground-penetrating radar for e-D sedimentological characterization of clastic reservoir analogs, *Geophysics*, **62,** 786–796.

Mukherjee, D., Heggy, E. & Khan, S.D., 2010. Geoelectrical constraints on radar probing of shallow water-saturated zone within karstified carbonates in semi-ardi environments, *J. appl. Geophys.*, **70,** 181–191.

Neal, A., 2004. Ground-penetrating radar and its use in sedimentology: principles, problems and progress, *Earth Sci. Rev.*, **66,** 261–330.

Olsen, H. & Andreasen, F., 1995. Sedimentology and ground-penetrating radar characteristics of a Pleistocene sandur deposit, *Sediment. Geol.*, **99**(1), 1–15.

Pedley, H.M., 1993. Sedimentology of the Late Quaternary tufas in the Wye and Lathkill valleys, North Derbyshire, *Proc. Yorks. Geol. Soc*., **49,** 197–206.

Pedley, H.M., Hil, I., Denton, P. & Brasington, J., 2000. Three-dimensional modelling of a Holocene tufa system in the Lathkill Valley, north Derbyshire, using ground-penetrating radar, *Sedimentology*, **47,** 721–737.

Pedley, M., 2009. Tufas and travertines of the Mediterranean region: a testing ground for freshwater carbonate concepts and developments, *Sedimentology*, **56,** 221–246.

Pedley, M. & Hill, I., 2003. The recognition of barrage and paludal tufa systems by GPR: case studies in the geometry and correlation of Quaternary freshwater carbonates, in *Ground Penetrating Radar in Sediments*, Vol. 211, pp. 207–223, eds Bristow, C.S. & Jol, H.M., Geological Society, London, Special Publication.

Pérez, A., Pueyo, O., Luzón, A., Muñoz, A. & González, A., 2012. Aplicación del georradar al estudio de sistemas fluviales tobáceos: los depósitos holocenos de Añavieja-Dévanos (Soria, NE de España), *Geogaceta*, **52,** 121–124.

Pratt, B. & Miall, A.D., 1993. Anatomy of a bioclastic grainstone megashoal (Middle Silurian, southern Ontario) revealed by ground-penetrating radar, *Geology*, **21,** 223–226.

Pueyo Anchuela, Ó., San Miguel, G., Martínez, V., Aurell, M. & Bádenas, B., 2012. Discriminación potencial de facies arrecifales por métodos geofísicos: aplicación a los pináculos arrecifales del Kimmeridgiense de Jabaloyas (Teruel), *Geogaceta*, **51,** 95–98.

Sbeinati, M.R., Meghraoui, M., Suleyman, G., Gomez, F., Grootes, P., Nadeau, M.J. & Al-Ghazzi, R., 2010. Timing of earthquake ruptures at the Al Harif Roman aqueduct (Dead Sea fault, Syria) from archaeoseismology and paleoseismology, *Geol. Soc. Am. Spec. Pap.*, **471,** 243–267.

Schenk, C.J., Gautier, D.L., Olhoeft, G.R. & Lucius, J.E., 1993. Internal structure of an eolian dune using ground-penetrating radar, *Spec. Publ. Int. Assoc. Sedimentol.*, **16,** 61–69.

Sigurdsson, T. & Overgaard, T., 1998. Application of GPR for 3-D visualization of geological and structural variation in a limestone formation, *J. appl. Geophys.*, **40,** 29–36.

Smith, D.G. & Jol, H.M., 1997. Ground penetrating radar investigation of the Peyto Delta, *Sediment. Geol.*, **113,** 195–209.

Stephens, M., 1994. Architectural element analysis within the Kayenta Formation (Lower Jurassic) using ground-probing radar and sedimentological profiling, southwestern Colorado, *Sediment. Geol.*, **90**(3/4), 179–211.

Tischer, G., 1965. Uber die Wealden-Ablagerung und die Tektonick der ostlichen Sierra de los Cameros in den nordwestlichen Iberischen Ketten (Spanien), *Geol. Jarhb. B*, **44,** 123–164.

Van Dam, R.L., 2001. Causes of ground-penetrating radar reflection in sediment, *PhD thesis*, Vrije Universiteit Amsterdam, 110 pp.

Van Dam, R.L., 2002. Internal structure and development of an aeolian river dune in The Netherlands, using 3-D interpretation of ground-penetrating radar, *Neth. J. Geosci.*, **81**(1), 27–37.

Van Dam, R.L. & Schlager, W., 2000. Identifying causes of ground penetrating radar reflections using time-domain reflectometry and sedimentological analyses, *Sedimentology*, **47,** 435–449.

Van Heteren, S., Fitzgerald, D.M., McKinlay, P.A. & Buynevich, I., 1998. Radar facies of paraglacial barrier systems: coastal New England, USA, *Sedimentology*, **45**(1), 181–200.

Vandenberghe, J. & van Overmeeren, R.A., 1999. Ground penetrating radar images of selected fluvial deposits in the Netherlands, *Sediment. Geol.*, **128,** 245–270.

Weill, P., Tessier, B., Mouazé, D., Bonnot-Courtois, C. & Norgeot, C., 2012. Shelly cheniers on a modern macrotidal flat (Mont-Saint-Michel bay, France)—internal architecture revealed by ground-penetrating radar, *Sediment. Geol.*, **279,** 173–186.

SUPPORTING INFORMATION

Additional Supporting Information may be found in the online version of this paper:

Figure S1. Evaluation of resolution of different GPR antennas attending the change in propagation velocity along the studied zone considering both radial resolution and first Fresnel zone radius. The information of the survey characteristics and configuration is also included for the different GPR profiles, antennas and surveyed zones (http://gji.oxfordjournals.org/lookup/suppl/doi:10.1093/gji/ggw167/-/DC1).

Please note: Oxford University Press is not responsible for the content or functionality of any supporting materials supplied by the authors. Any queries (other than missing material) should be directed to the corresponding author for the paper.